Journal of ELECTRICAL ENGINEERING, VOL 57. NO 8/S, 2006, 9-14

WIRELESS MAGNETIC FIELD SENSOR

Hans Hauser*— Johannes Steurer*— Johann Nicolics*— Laszlo Musiejovsky*— Ioanna Giouroudi*

A passive and wireless magnetic field sensor system based on the giant magnetoimpedance effect and surface acoustic wave technology is presented. First results show a sensitivity in the µT range and a bandwidth of 1.7 MHz. The application for remote non-destructive testing is proposed.

Keywords: giant magnetoimpedance effect, surface acoustic wave, amorphous wire, magnetic thin film

1 INTRODUCTION

Sensors based on magnetic principles are rapidly gaining importance for biomedical, industrial, automotive, and in-house applications. This is reflected by the increasing number of scientific and technical papers and books during the last decade, eg [1-5]. With the increasing number of sensors in a system on the one hand the number of interconnections for signal transmission and power supply is rising. On the other hand, conductive connections between sensors and measuring electronics are frequently related to problems in fulfilling requirements of electromagnetic compatibility, mechanical properties, and electric potential separation. In this field is a need for wireless sensor technology which can fully unfold its advantages only if the power supply is provided wirelessly too or if the sensor exhibits a passive operation principle.

The proposed principle is based on the giant magnetoimpedance (GMI) effect in thin amorphous wires or films [6, 7]. A new type of wireless surface acoustic wave (SAW) device provides an electrical load of one of the SAW reflectors by the impedance of a conventional sensor. In order to develop a wirelessly interrogable magnetic field sensor, the combination of low dimensional GMI structures and SAW transponders is performed. We expect a resolution of µT and a band width in the MHz range.

2 IMPEDANCE OF A GMI SENSOR

GMI sensors change their impedance as the magnetic field varies. Mostly the imaginary part of the impedance shifts towards lower values as the magnetic field rises. As our thin film structures are approximately 300 µm long the inductance is about 5 nH. In order to make measurements on this inductance the frequency must be at least some hundred MHz. In order to combine these sensors with SAW transponders only two frequencies are suitable. These are the available industrial frequency bands around 434 and 856 MHz. As our transponders work at 434 MHz all the measurement on the GMI elements are made at this frequency. The variation of the impedance dependent on the frequency and the magnetic field is shown in Fig.1.

At higher frequencies the impedance becomes more inductive and this inductance changes if a magnetic field

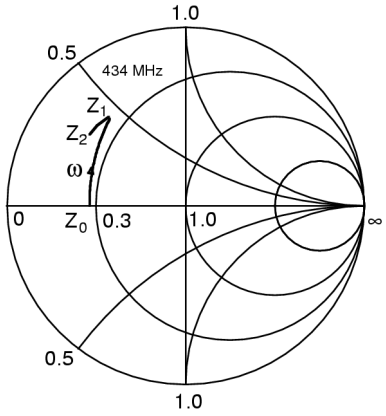

Fig. 1. Smithchart of the impedance variation of a GMI thin film structure Z_0 is the impedance with and without a magnetic field at low frequencies. Z_1 is the impedance at a frequency of 434 MHz without a magnetic field, Z_2 is the impedance in the presence of a magnetic field of 2 mT.

is applied. Considering one of our thin film GMI devices the impedance at 434 MHz is Z_1 = 11.62 Ω + j17.36 Ω without a magnetic field. It changes to Z_2 = 11.2 Ω + j16.17 Ω in the presence of a field of 1.4 mT. This means a difference in the inductance from 5.53 nH to 5.15 nH and an impedance change of 1.19 Ω. The phase change based on a magnetic field is $\Delta\varphi = 1.1°$.

3 OPERATING PRINCIPLE

SAW elements in combination with a sensor and an interrogation unit enable wireless installation, a completely passive operation and are maintenance free. They do not contain a battery, no charge storage, and no semiconductors. They are small, robust and can withstand extreme conditions [8]. Figure 2 shows a communication system including a SAW transponder together with a sensor and an interrogation unit connected using a radio link. The transmitter of an interrogator system sends a signal to a two port SAW transducer. This RF signal is received by the antenna of a SAW device and feed into an inter-digital transducer (IDT). Here a surface acoustic wave is excited, propagates along the substrate of the SAW and is partly reflected at each of the acoustic reflectors. In the first IDT the series of echoes of the acoustic waves are converted back into an RF signal and transmitted back. The second IDT is connected to variable external impedance (the GMI sensor) and changes the response of the

*Vienna University of Technology, Faculty of Electrical Engineering and Information Technology, Institute of Sensor and Actuator Systems, Gusshausstrasse 27-29/366, A-1040 Vienna, Austria, Email: hans.hauser@tuwien.ac.at

ISSN 1335-3632

IDT in magnitude and phase. The receiver in the interrogator system receives this signal, evaluates its magnitude and phase and gains information about the sensor.

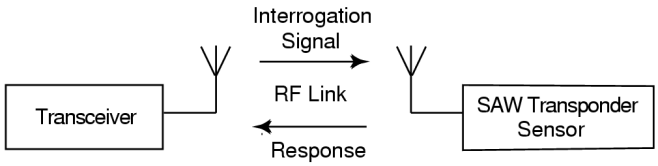

Fig. 2. Sensor interrogation system

Figure 3 shows the schematic layout of a SAW transponder connected to load impedance in our case a GMI sensor. An RF burst is transmitted from the interrogation unit and received by the antenna of the SAW element. The inter-digital transducer of the SAW converts the incoming burst to a surface acoustic wave. It propagates towards the reflectors of the SAW. The reflectors are placed in distinct displacements and reflect the incoming wave towards the antenna. The interrogation unit receives this signal (a pulse train) and gains the information about the reflectors. Mainly it evaluates magnitude and phase, respectively the I- and Q-information.

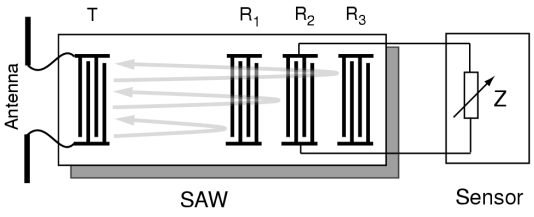

Fig. 3. Schematic layout of the SAW Transponder and a load impedance, eg the GMI wire

Our SAW elements are built as two-port devices. One port (T) is connected to the antenna, the other (R_2) is connected to the sensor. They act as reflective delay lines using three different reflectors, two as references and one as a IDT connected to the GMI sensor. The two reference reflectors (R_1, R_3, both not loaded) are used to circumvent the ambiguity of the phase and to consider the temperature coefficient. $LiNbO_3$ substrates have a phase velocity temperature coefficient of 85 ppm/K. Other unwanted influences are mechanical stress, pressure or acceleration.

The middle reflector (R_2) is implemented as an inter-digital transducer too and is loaded with a varying impedance (the GMI sensor). The variation of the load impedance changes the acoustic transmission and reflection properties. This changes the amplitude and the phase of the received signal. Two reflectors are sufficient but three yield a higher accuracy of the measurement system. Figure 4 shows the realized SAW structure. The IDTs are easily seen. Outside of the IDTs there are electrical and mechanical adsorbers to suppress further reflections.

The layout of the SAW element must be done in accordance with the propagation time of the acoustic wave. In our case the first reflector is 3 µs away from the antenna IDT, the second (loaded) reflector (R_2) is 1 µs away from the first reflector and the third reflector is 1 µs away from the second reflector. So the first burst returns to the antenna after 6 µs and the third burst arrives the antenna after 10 µs. These two times determine the receiver window. Outside of this window all the received signals must be suppressed to avoid interference.

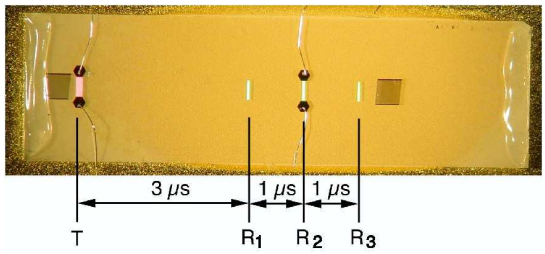

Fig. 4. Photo of the SAW element. Mechanical adsorbers are placed at both ends of the chip. Electrical adsorbers are near the IDT T and IDT R_2. The antenna IDT T at the left and the three reflectors R_1, R_2, R_3 in the middle of the sensor are visible on the chip too.

The impedance of the GMI sensor was transformed to the impedance of the IDT to achieve a high phase change in the reflected burst. Figure 5 shows the acoustic reflectivity of the IDT as a function of the load impedance. The processing of phase changes is more accurate and easier to do than evaluating the magnitude of the signal.

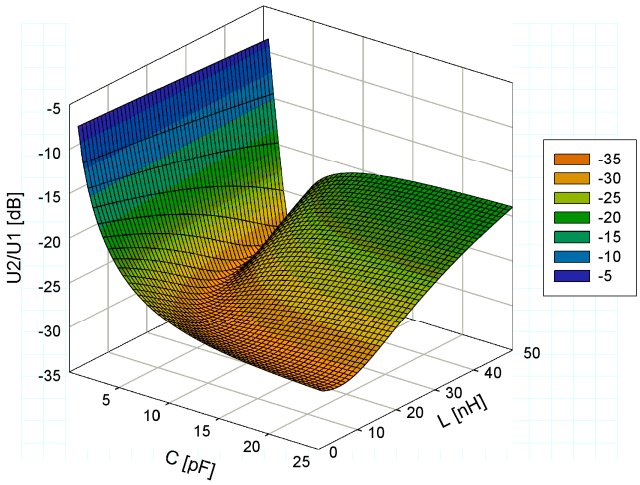

Fig. 5. Variation of the magnitude of the acoustic reflection coefficient (vertical axis, in dB) as a function of the series impedances L_{GMI+M} (right axis, in nH) and C_S (left axis, in pF). The series resonant frequency is easy to see as valley. Here, the phase change is at a maximum.

Our SAW devices have an input impedance of 28.5 Ω - j13.6 Ω. At 434 MHz this is equivalent to a resistor of 28.5 Ω in series to a capacitance of 72.0 pF. The output impedance is 36 Ω - j72.5 Ω which is represented by a resistor of 36 Ω in series to a capacitor of 5.1 pF.

In order to use the GMI thinfilm sensors together with the SAW transponder a matching of the impedance of the GMI sensor to the output impedance of the SAW transponder is necessary (see Fig. 6). An essential measurement requirement is a high sensivity to magnetic fields.

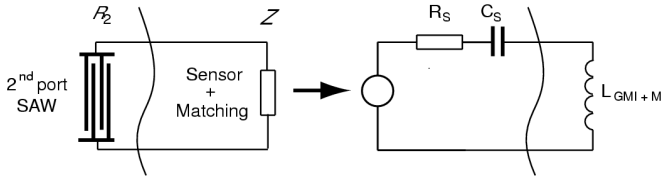

Fig. 6. Series equivalent circuit of the 2nd port of the SAW transponder (R_S, C_S) and the GMI element L_{GMI} including the matching inductance L_M

The higher the frequency the better the sensivity of the GMI element as shown in Fig. 1. As the operating frequency is specified only the operating point of the impedance mating of the two devices can be varied. Figure 5 shows the reflection coefficient of the SAW transponder as a function of the internal impedance of the SAW element and load impedance (GMI sensor). At the resonant frequency the plane of the reflection coefficient shows the sharpest change, eg changes of the impedance of the GMI sensor cause a great change of the reflection coefficient of the second port of the SAW transponder. This implicates a high variation of the reflection of the interrogation burst.

In case of a reflective delay line, if one IDT is connected to the antenna and the other IDT is open circuit, then all the incoming energy is reflected to the antenna. If the other IDT is in series resonance then all the energy is dissipated in the SAW. So tuning the load impedance the reflectivity of the IDT can be adjusted in magnitude and phase. The reflectivity P_{11} in Eq. (1) of a two port split-finger IDT as a function of a termination impedance Z is computed and evaluated in [9] and [11]:

$$P_{11} = \mathrm{Re}(P_{33}) / (P_{33}+1/Z) \; . \qquad (1)$$

P_{33} is the reflection coefficient at the electrical port 3 (other acoustic ports open), Z is the load impedance in our case the GMI sensor. Figure 7 shows the changes in the magnitude and phase of the reflectivity P_{11} as a function of the load impedance Z (GMI sensor).

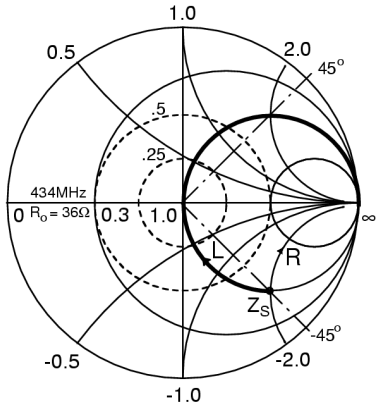

Fig. 7. The smith diagram shows the reflection coefficient P_{11} of the loaded IDT at varying load impedances. The dashed lines show circles of constant reflection coefficient. Z_S is the output impedance of the IDT. If an inductive load reaches point (1,0) of the diagram the IDT is at series resonance.

These facts are evaluated in Fig. 5, too. Here the valley represents the series resonant frequency as a function of the capacitance and the inductance of the GMI element and the matching inductance L_{GMI+M}.

4 MEASUREMENT SYSTEM OVERVIEW

In order to communicate with the GMI-sensor combined with the SAW-element a transceiver is necessary. The transmitter sends out a burst which excites the SAW-element, the impedance of the coupled GMI-sensor changes the characteristic of the reflected burst. The SAW-element works as a reflective delay line which reflecting coefficient is varied by the impedance of the GMI-sensor. Figure 8 shows a typical response of the SAW element. The received burst is compared to the received one by measuring amplitude and phase changes. To compensate against temperature changes and mechanical strain two additional reflectors are added in the SAW-element. These reflected bursts are used as a reference too.

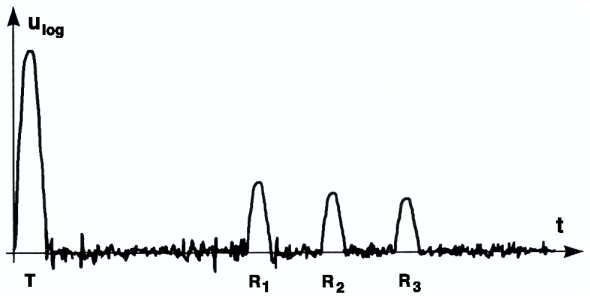

Fig. 8. Impulse response of the SAW. T is the interrogation signal, 6, 8, and 10 µs later the responded bursts (R_1, R_2, R_3) return; the output of the logarithmic amplifier is U_{log} (demodulated RF burst)

We used the 434 MHz band of the possible industrial, scientific and medical radio bands (ISM) because the devices are more easy to manufacture and the components are readily available. The maximum bandwidth allowed is 1.7 MHz. SAW elements are manufactured using one lithography process only (Al sputtering and etching). The acoustic wave propagates for a factor of 10^5 slower than an electromagnetic wave. Using this frequency, $2 \cdot 10^5$ acoustic wavelengths are stored. The SAW resonator shows a typical loaded quality factor Q of about 10^4. The measurement system consists of SAW element combined with a GMI sensor (wire or thin film element), a transceiver and an analyzing unit.

The interrogation system is characterized by the generation of a short RF burst, a corresponding receiver unit, coherent phase detection and a fast sampling unit. The data is calculated off line. The transceiver for the SAW transponder system is constructed based on pulse radar and is shown in Fig. 9.

A local oscillator operating at 418 MHz and an oscillator of 16 MHz are mixed (Mix 1) in order to generate the

434 MHz transmission burst. This kind of signal generation must be done due to the need of a coherent detection. The received signal is amplified in a 16 MHz IF stage and then synchronously demodulated using the 16 MHz oscillator. The higher of the two sidebands out of the mixer 1 is feed throw a band-pass filter and then switched on and off to generate the RF burst (T). The burst is 1 µs long. A preamplifier and a power amplifier boost the burst to an RF level of 20 dBm. This signal is feed via transmit-receive switch (TxRx switch) to the antenna.

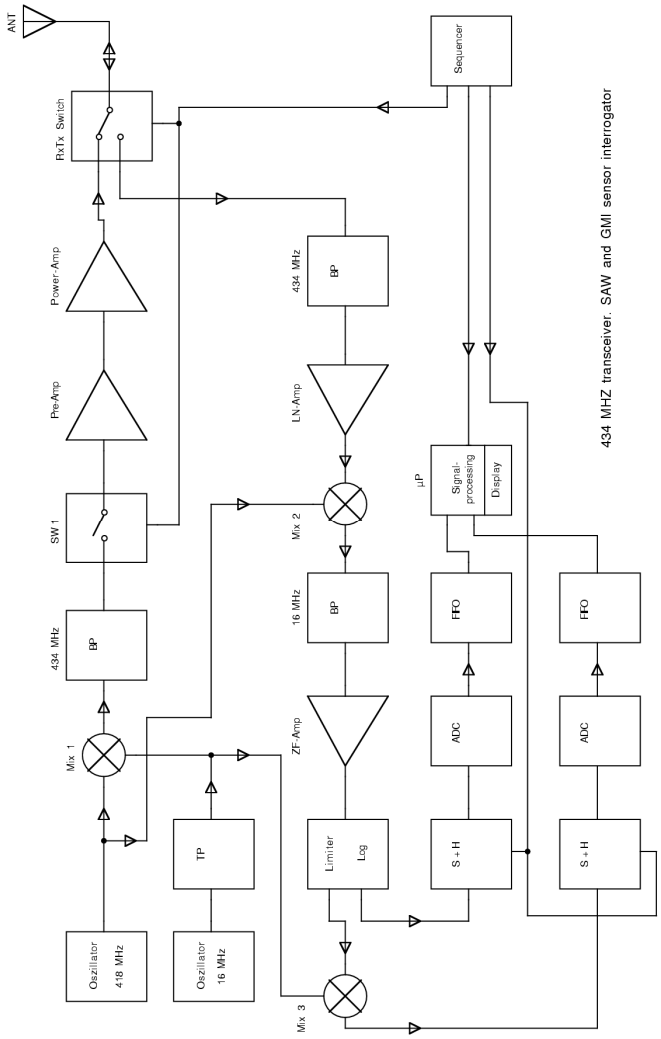

Fig. 9. Overview of the transceiver unit.

The receiver part is realized as a heterodyne receiver using a 16 MHz IF stage. The reflected SAW echoes (R_1, R_2, R_3) pass a band-pass filter and a low noise amplifier. In the following mixer stage (Mix 2) the received bursts are converted down to the IF of 16 MHz. The IF amplifier consists of a logarithmic amplifier and a limiter. The log amplifier delivers the magnitude of the signal while the limiter provides the phase information. The system operates fully coherent with respect to the local oscillators so many RF samples can be summed up to enhance the signal-to-noise ratio. Figure 10 sketches the idea of the coherent detection. This feature greatly increases the readout distance, because the receiving signal level decreases with the fourth power of the distance (radar equation).

The magnitude and the phase output are sampled in two corresponding sample and hold circuits in fact they are simultaneously converted to DC three times (R_1, R_2, R_3). Each sample passes an AD converter and is fed into a FIFO. Here the signal processing unit fetches the samples. They are stored, processed and evaluated in the data acquisition circuit. After the signal processing is done a new cycle starts. The required cycle time of the ADC unit is about 1 µs. Because the whole system is coherent all the information contained in the phase is conserved. Since the magnitude and phase are constant during the sample window no extremely fast digital signal processing is necessary.

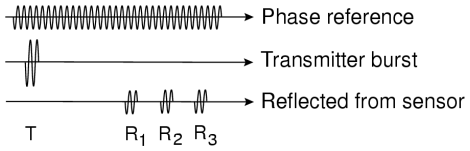

Fig. 10. The transmitted burst T and the received bursts R_1, R_2, R_3 have a distinct phase reference hence a coherent demodulation is possible

The sequencer generates the different windows. In order to eliminate the interrogation signal itself and all environmental echoes at the receiver the first 3 µs after the transmitter burst must be gated. The transmitted burst (transmit window) is 1 µs long, the receiver is active 5 µs after the outgoing bust and has a duration of 6.5 µs (receiving window). During this window each response of the three reflectors in the SAW element is sampled and stored in the FIFO. Outside this receiver window the receiver is disabled.

The receiving level at the receiver decreases, in accordance to the radar equation, with the fourth power of the distance between the SAW and the transmitter. The maximum distance r is given by the transmitted power P_0 of the transmitter, the gain of the two antennas G_r, G_s, the insertion loss of the SAW and the conversion gain of the sensor element D; kT_0BF is the thermal noise power and λ the electrical wavelength. SNR is the desired signal to noise ratio:

$$r = 1/4\pi \, [(P_0 \, G_r^2 \, G_s^2 \, \lambda^4) \, / \, (\, kT_0BF \, D \, SNR)]^{1/4} \qquad (2)$$

The maximum transmitted power is limited to 15 dBm. The insertion loss D of the SAW depends on the operating frequency and is in the range of 14…20 dB. This loss consists of the matching loss at the antenna IDT and the transducer losses. Because of the adsorbers near the IDT the acoustic wave travels in one direction only and gains 2 x 3 dB compared to a single port device. The antenna gains are about 3 dB. Depending on the signal processing the signal to noise ratio (SNR) should be at least 10 dB. Under these pre-assumptions the maximum operating distance is 2.5 m in the 434 MHz band. An estimation of the

losses in SAW devices is given in [10]. Using coherent signal integration or directive antennas a distance up to 10 m is possible.

5 FIRST RESULTS

The GMI wire and the matching capacitance was connected to the IDT2 port of a SAW chip. The field B_0 was applied by an electromagnet. The results, the amplitude A_{IDT2} of the affected reflector relative to the reference reflector amplitude A_{ref}, are shown in Fig. 11. This relative amplitude is defined as

$$A_{rel}(dB) = 20 \log | A_{IDT2} / A_{ref} | \quad (3)$$

The sensitivity (A_{rel} / B_0) is 80 dB/T in the region of weak fields (up to 30 mT). The measurements have been carried out using a 13 mm long amorphous FeCoSiBNd wire with 30 µm diameter. The uncertainty depends also on the SNR, which is depending on the distance between SAW and transceiver unit. For a 2 m distance the reproducibility was about 5 %.

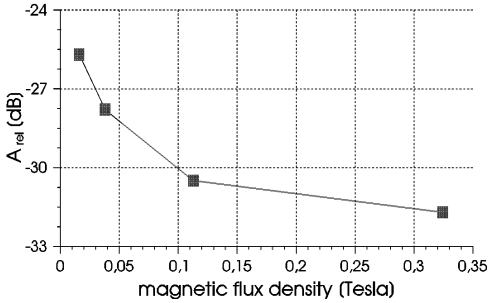

Fig. 11. Amplitude of the impedance affected reflection relative to the reference, A_{rel} versus applied magnetic flux density B_0.

6 CONCLUSIONS

The developed sensor system provides passive and wireless operation combined with moderate sensitivity and SNR in first results. One of the main applications could be a highly innovative non-destructive evaluation method for monitoring ferromagnetic constructions: The passive sensor chip is placed close to ferrous parts, eg, reinforcement within concrete and it will be wirelessly requested by a RF pulse. Thus the change of the magnetic stray field due to degradation by oxidizing or stress could be detected by periodical control during the whole lifetime of the construction. A collapse of buildings, bridges, etc, could be avoided by early warning.

Acknowledgements

Financial support was granted (no. 16698N-02) by the "Fonds zur Förderung der Wissenschaftlichen Forschung". The authors are grateful to Prof Evangelos Hristoforou for providing the GMI wire samples as well as to Günther Stangl and Dr Robert Medek for their technical support.

REFERENCES

[1] ROUMENIN, C. S.: Solid State Magnetic Sensors. Elsevier, Amsterdam 1994.

[2] MALLINSON, J. C.: Magneto-Resistive Heads. Academic Press, San Diego 1996.

[3] COMSTOCK, R. L.: Magnetism and Magnetic Recording. John Wiley, New York 1999.

[4] RIPKA, P.: Magnetic Sensors and Magnetometers. Artech House, Boston 2001.

[5] TUMANSKI, S.: Thin Film Magnetoresistive Sensors. Institute of Physics, Bristol, 2001.

[6] GIOUROUDI, I. — HAUSER, H. — DAALMANS, G. — RIEGER, G. — WECKER, J.: Characterization of Magneto-Impedance Thin Film Microstructures. J. Electrical Engineering 55, no 10/S (2004), 11–15.

[7] GIOUROUDI, I. — HAUSER, H. — MUSIEJOVSKY, L. — STEURER, J. — DIDOSYAN, Y.: Investigation of Magnetoimpedance Effect in Amorphous Thin-Film Microstructures. J. Appl. Phys. 97 (2005), 10M109-1 – 10M109-3.

[8] REINDL, L. — SCHOLL, G. — OSTERTAG, T. — SCHERR, H. — WOLFF, U. — SCHMIDT, F.: Theory and application of passive SAW radio transponders as sensors. IEEE Trans. UFFC 45, No. 5, (1998), 1281-1292.

[9] TOBOLKA, G.: Mixed matrix representation of SAW-transducers, IEEE Trans. Sonic Ultrason. 26 No. 3 (1979), 426-428.

[10] RÖSLER, U. — COHRS, D. — DIETZ, A. — FISCHAUER, G., RUILE, W. — RUSSER, P. — WEIGEL, R.: Determination of leaky SAW propagation, reflection and coupling on $LiTaO_3$. Proc. IEEE Ultrasonics Symp. (1995), 247-250.

[11] RUILE, W.: P-Matrix Modelle von Oberflächenwellen-Bauelementen. PhD thesis, TU München 1994.

Received 13 November, 2006

Hans Hauser (Prof, PhD) is associated professor with the Vienna University of Technology. He was educated in Austria and received the Dipl.-Ing. (MSc) in Electrical Engineering and in 1999 he became the head of the Institute of Material Science in Electrical Engineering. From 2000 to 2002, he was the head of the Institute of Industrial Electronics and Material Science at the Faculty of Electrical Engineering and Information Technology. He is a IEEE Senior Member and member of the board of the "TU Vienna Magnetics Group". From 1998 to 2003, he coordinated one of the faculty's top priorities, "Sensors and Packaging". He is consultant for several companies in Europe and member of the board at international conferences and scientific publishers. He gives courses on material science and fundamentals of electrical engineering. His research topics include magnetic materials, dielectrics, superconductors, and materials aspects of sensors.

Johannes Steurer (PhD) joined the Institut für Allgemeine Elektrotechnik in 1980 and worked on RF communication systems for biomedical implants. Since joining the Biosensors Group in 1987, he has been responsible for the development of the test equipment for various micro sensors and the telemetry systems. His research interests include factor analytic computations as well. He received his Dr. techn. degree in electronics engineering from the Vienna University of Technology in 1985. Additionally, he holds a PhD in biology and a Dr. rer.soc.oec. in eco-

nomics from the University of Vienna. He teaches courses in analogue circuit design and is a lecturer at the University of Applied Arts in Vienna.

Johann Nicolics (Prof, PhD) graduated in electrical engineering in 1980 and received the PhD degree in 1988 from Vienna University of Technology, where he is professor since 1996. He set-up a research group on electronic packaging and is now the head of the department of Applied Electronic Materials at the Institute of Sensors and Actuator Systems. His research interests cover laser material micro-processing, especially laser soldering, printed circuit manufacturing processes, thermal management in power electronics, and many other topics in the field of electronic packaging. He has authored and co-authored more than 150 scientific publications in technical journals, conference proceedings and book contributions and he is senior member of IEEE.

Laszlo Musiejovsky (PhD) graduated in electrical engineering at the Budapest University of Technology and Economics, Hungary, in 1990. He was assistant teacher and researcher in the electronics packaging group at the Institute of Industrial Electronics and Material Science at the Vienna University of Technology. His current research interests focus on material processing with laser and on thermal modelling.

Ioanna Giouroudi (PhD) received the degree of Doctor of Science from the Vienna University of Technology, Austria, in 2006 and her degree in Electrical Engineering from the Technological Educational Institute, Chalkis, Greece, in 2003. She held a Marie Curie Fellowship and was working in the field of Handling and Assembly in Micro-technology. Her research interests are magnetic materials, giant magneto-impedance sensors, micro-handling systems for MEMS applications, micro-joining systems, micro-robotics.